

## Earthquake Simulation in Virtual Metropolis

### Using Strong Motion Simulator and Geographic Information System

#### 強震動シミュレータと地理情報システムを組み合わせた地震シミュレーション

Fang YANG\* Tsuyoshi ICHIMURA \*\* and Muneo HORI\*\*\*

楊 芳・市村 強・堀 宗朗

\* Student, Earthquake Research Institute, University of Tokyo, (Yayoi, Bunkyo, Tokyo 113-0032)

\*\* Member, Dr. Eng., Research Assoc., Dept. of Civil Engineering, Tohoku University, (Aobayama 06 Sendai, Sendai, 980-8579)

\*\*\* Member, Ph.D., Professor, Earthquake Research Institute, University of Tokyo, (Yayoi, Bunkyo, Tokyo 113-0032)

Realistic simulation of a possible earthquake is important for making rational plan against earthquake disasters. This paper proposes such a simulation method using a high resolution strong motion simulator and constructing a computer model of a whole city. The data for the model are provided by certain Geographic Information System, and underground structures and each building are modeled. The methodology of constructing these models is studied, since available data are usually limited. An example of a city model is constructed and earthquake simulation is made to examine the basic usefulness of the simulation.

*Key Words: Earthquake Simulation, Computer Model for Metropolis, Strong Motion Computation, Geographic Information System*

### 1. Introduction

Past huge earthquakes which hit metropolises resulted in serious damage in human lives and estates as well as social infrastructures. To achieve more safety for an earthquake, it is essential to predict possible disaster in a more realistic manner. Such predication contributes to making more rational counter measures.

To realize this predication, we need the high accuracy for strong motion simulation and the reliable and effective models of the target metropolis. However, there are two difficulties in such earthquake simulation. The first is the requirement of huge computer resources; see Ichimura and Hori<sup>1),2)</sup>. The second is that data for underground structures (geological and ground) and structures (lifelines, buildings, etc.) are limited. While the simulation methods are being developed and advanced methods are being proposed, less studies are made on the construction of a numerical analysis model for undergrounds and structures by making use of available but limited data, which, for a larger city, are (or will be) stored in certain Geographical Information

Systems (GIS's).

The authors are proposing an earthquake simulation by combining the strong motion simulator with GIS's. The strong motion simulator is being developed to compute the distribution and time series of the strong motion with the high spatial and temporal resolution. The GIS's are used to construct analysis models for undergrounds and structures, to which the computed strong motion is applied and the resulting response of the structures are computed. The key issue is the construction of analysis models using the GIS data.

In this paper, we propose a methodology of automatically constructing such analysis models, and demonstrate an earthquake simulation of combining the strong motion simulate with the models constructed from the GIS data. First, we explain the methodology of the model construction in Section 2. Data which are required and available for the model construction are summarized. Next, in Section 3, we construct a so-called virtual town using the actual GIS data for Roppongi Area, Tokyo, Japan; the virtual town has analysis models for both the underground structures and around 150 buildings. For given

Table 1. Data required for analysis models and data currently available in GIS's.

	required	available
underground structure		
configuration	boundary depth soil type, etc.	elevation data(50m[m] mesh GIS data) borehole data
material properties	density wave velocity non-linear properties	database for soil type- material parameter relation
structure		
basic	location structure type	digitized perspective view
configuration	structure dimension member dimension	height data (satellite image)
material properties	member elastic property member non-elastic property	none

earthquakes, the resulting strong motion near the ground surface and the dynamic responses of all buildings are computed, and it is shown that the structure response varies from place to place, as well as for a given earthquake, in a very wide range.

## 2. Modeling Virtual Town

A virtual town (or a virtual metropolis if large) is a set of numerical analysis models for the underground structures and the structures and the buildings located in a target town. We summarize data required for these analysis models and data currently available in GIS's in Table 1. The discrepancy between the required and the available data is owing to the fact that the analysis models are for mechanical computation and need mechanical information such as configuration and material properties, while the GIS is originally developed for the geographical purposes such as the land usage and the land arrangement. As is seen, data for constructing the underground models are limited, if surface layers are complicated (which is often a case due to the sedimentation processes in geological time scale). On the other hand, digital data for constructing the structure models exist if the target structure is designed in a Computer-Aided-Design (CAD) system.

In this section, we present the methodology of modeling the virtual town by making use of the GIS data. For the underground structures, we do not expect that GIS of larger quantity and better quality data will be available, and hence we made the methodology suitable for the current GIS data. For the structures, the situation will be changed if CAD is spread and owners provide the CAD data. Thus, we develop a relatively simple methodology which is suitable to a case when CAD data are not available.

### 2.1 Ground structure model

A model of stratified soil layers is used for the underground structures of the virtual town. The configuration

and the material properties of each layer need to be determined. In general, the estimation of the layer configuration is difficult mainly because available borehole data are limited (or the density of boring sites is sparse) and even adjacent borehole data are often inconsistent; the inconsistency means that the sequence, not the thickness, of distinct layers differs; see Fig. 1.

#### (1) Estimation of soil layer sequence

We first develop a method of estimating the soil layer sequence. While there are various methods are proposed for this purpose, most of them are for a case when few boring sites are available and not suitable for a case when many but inconsistent borehole data are given. Thus, the developed method is robust and can automatically correct the inconsistency of the borehole data. The procedures of estimating the soil layer sequence according to the proposed method is summarized as follows:

- i. Pick up one bore-hole data, and set the layer sequence as the initial reference sequence.
- ii. Compare the layer sequence of adjacent bore-hole data with the reference sequence.
  - ii-a. If it matches, go to the next bore-hole data.
  - ii-b. If it does not match, combine the two sequences to make new reference sequence that is consistent with them. At this stage, the thickness of some layers can be zero.
- iii. Repeat ii until all borehole data have a common consistent layer sequence.
- iv. Determine *major* layers whose average thickness is larger

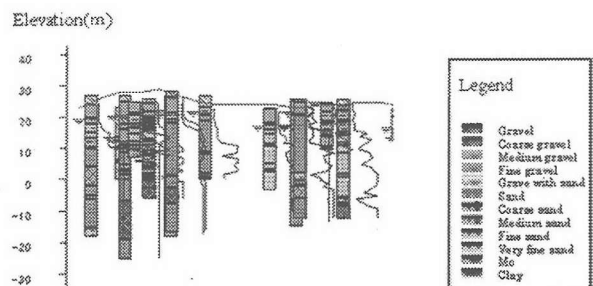


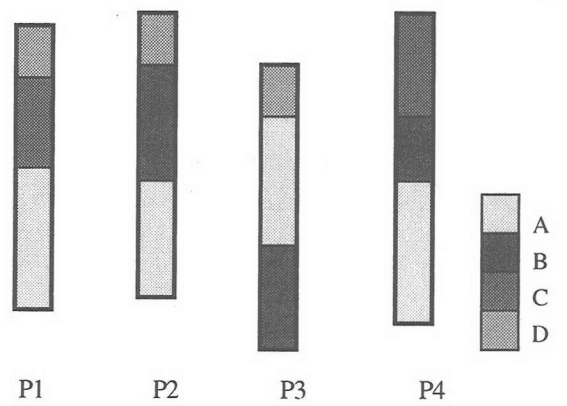
Figure 1. Example of neighboring borehole data.

than a pre-determined value among all layers in the reference sequence. Omit the thinner layers, and the layer sequence is finalized.

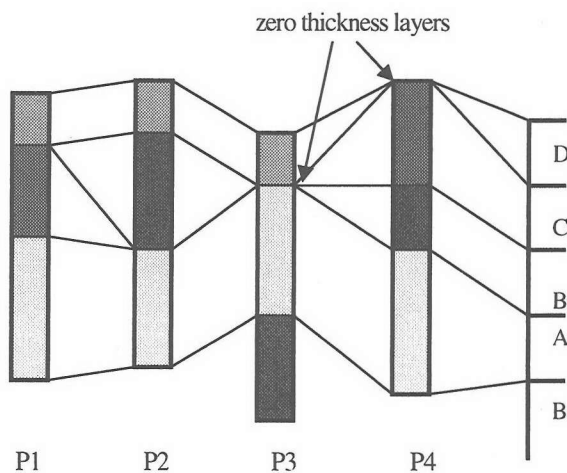
We explain this procedure using an example of bore-hole data, P1~P4, as shown in Fig. 2. We first choose P1, and D-C-A as the initial reference sequence (i). Comparing P2 data, we modify the reference as D-C-B-A, and add zero thickness B and C layers to P1 and P2, respectively (ii). Repeating this modification, we have D-C-B-A-B as the reference sequence (iii). If the average thickness of the last B layer is smaller than a pre-determined, we omit this layer and finalize the sequence of the major layers as D-C-B-A (iv).

**(2) Interpolation of layer thickness**

Once the layer sequence is determined, we have to estimate the layer thickness, interpolating the borehole data. We employ a grid algorithm<sup>3)</sup>, in which continuous distribution of thickness is replaced by discontinuous grid values. In this algorithm, the constraint condition is given as:



a) neighboring borehole data



b) estimation of layer sequence

Figure 2. Example of borehole.

$$s(x_k, y_k) - z_k = 0 \tag{1}$$

where  $z_k$  is the elevation at borehole data,  $s(x_k, y_k)$  is given as:

$$s(x_k, y_k) = c_1(x_k, y_k)f_{ij} + c_2(x_k, y_k)f_{i+1j} + c_3(x_k, y_k)f_{i+1j+1} + c_4(x_k, y_k)f_{ij+1}$$

here  $c_{1-4}$  are bi-linear weight functions; see Fig. 3.

The grid algorithm then finds a set of  $\{f_{mn}\}$  which minimizes:

$$J = \int |\nabla f|^2 ds + m \int |\nabla^2 f|^2 ds \tag{2}$$

subject to constraints of  $\{f(x^k) = f^k\}$  with  $f^k$  being the  $k$ -th measured value of  $f$ . Here, the first and second integrands are the square of the gradient and curvature norm of  $f$  and  $m$  is the weight between them.

In numerical computation, we apply the multi-grid method to efficiently determine  $\{f_{mn}\}$ . This method first use coarse grid to discrete  $f$  and gradually increase the fineness of the grid.

**2.2 Structure (building) model**

A structure model ranges from a simple linear model such as one-degree-of-freedom system to a sophisticated non-linear model used in the finite element method computation. The linear model is enough if the structure is safe to the given strong motion (i.e., remains in the elastic response regime). The non-linear model is required if the structure reaches non-linear regime and has a possibility of local or total collapse.

The CAD data are useful in constructing the complicated non-linear model for a target structure. If such data are not available, the alternative is to use a simple linear model; at least whether the structure remains in the elastic regime or not is examined by using this model. In this section, we focus on buildings, and develop a method of constructing a linear multi-degree-of-freedom (MDOF) system model for them by using GIS data.

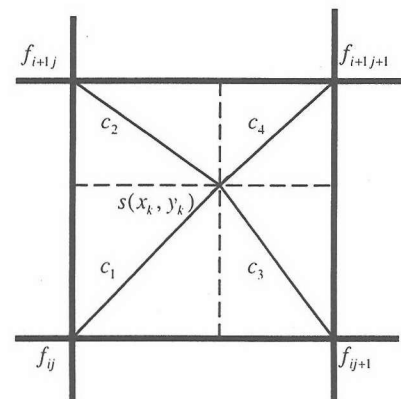


Figure 3. Bi-linear interpolation inside grid.

Table 2. Dynamic properties of different buildings.

Materials	$T_1$ (sec.)	$\xi_1$
WH	0.2–0.7	0.02
RC	$T_1=0.02H$	0.03
SRC	$T_1=0.03H$	0.02

**(1) Data needed for linear model**

The configuration of the MDOF system, or the number of the degree-of-freedom ( $N$ ), as the story number, is available in GIS data. While few GIS data available for the building height,  $H$ , we can estimate the height from  $N$ . Assuming the average height of one floor as 3.5[m], we can thus determine the total height, i.e.

$$H = 3.5 \times N, \tag{3}$$

The mechanical properties of the MDOF system need to be determined. According to the design code and statistical data 4), 5), 6), 7), 8) and 9) of building structures, the period ( $T_1$ ) and the damping ratio ( $\xi_1$ ) of the fundamental vibration mode can be estimated from the building height  $H$ . Table2 shows the estimate of  $T_1$  and  $\xi_1$  for three building types, namely, wooden-house (WH), RC building (RC) and SRC building (SRC).

It is known that for a shorter building ( $T_1 < 0.5$ [sec]), the effects of higher modes need not to be considered. For a higher buildings ( $T_1$  takes a value of several seconds), we should account for higher modes. In general, it is enough to compute up to the third or fourth mode<sup>7)</sup>. There is an established relationship between the fundamental period  $T_1$  and the second and third periods,  $T_2$  and  $T_3$ , as follows:

$$T_2 = 1/3T_1 \text{ and } T_3 = 1/5T_1. \tag{4}$$

Also, the following recursive formulae are known to the damping ratio of  $n$ -th and  $n+1$ -th modes ( $\xi_n$  and  $\xi_{n+1}$ )<sup>9)</sup>:

$$\xi_{n+1} = 1.4\xi_n \text{ for RC, } \xi_{n+1} = 1.3\xi_n \text{ for SRC.} \tag{5}$$

WH, which is categorized as a shorter building, does not have to consider higher modes.

If a building is modeled as a lump-mass MDOF system, we need to determine the ratio of the lumped mass and the spring constant,  $m/k$ , such that, together with these periods, the mode shapes ( $\Phi_n$ ) can be estimated. We take advantage of the

fact that the fundamental mode  $\Phi_1$ , is approximately given to an  $N$ -floor building<sup>10)</sup>. By definition<sup>11)</sup>, we have:

$$\frac{4\pi^2}{T_1^2} = \frac{\Phi_1^T K \Phi_1}{\Phi_1^T M \Phi_1} \tag{6}$$

where  $\Phi_1$  is the approximate fundamental mode vector and  $K$

and  $M$  are the stiffness and mass matrix given as:

$$K = k \begin{bmatrix} 2 & -1 & \dots & 0 \\ -1 & 2 & \dots & 0 \\ \vdots & \vdots & \ddots & \vdots \\ 0 & 0 & \dots & 1 \end{bmatrix} \text{ and } M = m \begin{bmatrix} 1 & 0 & \dots & 0 \\ 0 & 1 & \dots & 0 \\ \vdots & \vdots & \ddots & \vdots \\ 0 & 0 & \dots & 1 \end{bmatrix} \tag{7}$$

Thus, we can estimate the value of  $m/k$ .

**(2) Approximate modal analysis for MDOF system**

Once necessary mechanical properties of the MDOF system are estimated, we carry out simple modal analysis to estimate the dynamic responses of the target buildings. Since the target vector differential equation is

$$M\ddot{v} + C\dot{v} + Kv = -M\ddot{z}, \tag{8}$$

where  $v$  is the displacement vector and  $z$  is linear to a vector  $(1,1,1,\dots,1)^T$ . If  $v$  is decomposed as:

$$v = \sum q_n \Phi_n, \tag{9}$$

with  $\Phi_n$  is the  $n$ -th mode shape, the coefficient  $q_n$  must satisfy:

$$\ddot{q}_n + 2\xi_n \omega_n \dot{q}_n + \omega_n^2 q_n = -(M^{-1/2} \Psi_n)^T (M\ddot{z}), \tag{10}$$

where  $\omega_n$  is the natural frequency corresponding to the period  $T_n$ . Thus, we can numerically compute the structure response for a given ground motion. Indeed, if  $z_g$  is the scalar ground motion, we have:

$$v = \sum Q_n (\sum \Psi_{ni}) \Psi_n, \tag{11}$$

where  $Q_n$  is the solution of (10) when the right side is replaced by  $z_g$ , and  $\Psi_n$  is the normalized mode shape ( $\Phi = M^{-1/2} \Psi_n$ ). As is seen, we do not have to know the value of  $m$  (or  $k$ ) in computing the response vector  $v$ .

**3. Strong Motion Simulator using Macro-Micro Analysis Method**

A prototype of a strong motion simulator has been developed. This simulator is based on the macro-micro analysis method that takes advantage of the multi-scale analysis for efficient and accurate numerical computation and the bounding medium theory for constructing a reliable model. Wave propagation processes from fault to ground surface can be computed with sufficiently high spatial and temporal resolution; see Ichimura and Hori<sup>1),2)</sup>.

The multi-scale analysis of the macro-micro analysis method uses spatial coordinates of different length scales. The macro-analysis and the micro-analysis are set for computing the

wave propagation in the geological scale with low resolution and in each town or ward with high resolution, respectively. The uncertainty of geological and ground structures is resolved by considering a stochastic model, which prescribe stochastic distribution of structure configuration and mechanical properties, such as the mean and the variance. The bounding medium theory is used to make fictitious but deterministic models for the stochastic model such that the mean responses of the stochastic model can be bounded by the responses of these deterministic models.

The prototype of the strong motion simulator is able to compute the strong motion distribution with high special and time resolution, say, a few meters and a comma few seconds. Such resolution is needed for the dynamic analysis of structures whose natural frequency goes up to a few Hz. Also, in this resolution, the wave amplification near the ground surfaces that consists of soft layers is computed accurately, and some sharp three-dimensional topographical effects on the amplification can be obtained.

#### 4. Example of Earthquake Simulation in Virtual Town

As an example of earthquake simulation, we construct a virtual town for an area near the previous building of Institute of Industry Science, University of Tokyo, in Roppongi. The target area is shown in Fig.4; the center is: (139.731706306E, 35.661915222N) and the domain is 300x300[m].

First, we explain the construction of the virtual town, i.e., the underground structure model and the building models. The underground structure model is presented in Fig. 5; the depth of the model is 60[m]. There are six major soil layers in this model. Since only two boring sites are located in this area, an area of 1000x1000[m] is analyzed to determine the layer configuration. Fig. 5 shows the boring sites and an example of interface configuration between the fifth layer and the bedrock mass. Also, Table 3 gives the characteristics of each layer and the bed rock on which these layers are located.

The MDOF system is constructed for each of around 140



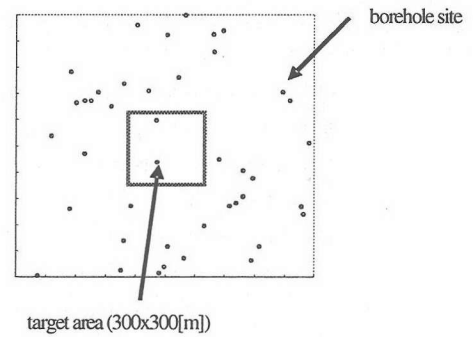
Target Area (300x300[m])

Figure 4. Target.

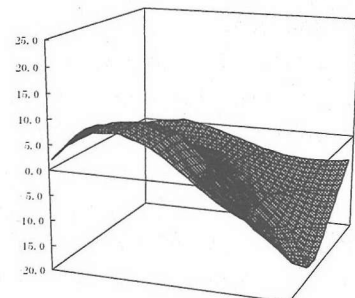
Table 3. Characteristics of soil layers.

Number of layer	Soil type	Density [g/cm <sup>3</sup> ]	S wave velocity [m/s]	P wave velocity [m/s]
1	Surface soil	1.625	120.0	204.0
2	Loam	1.550	135.0	229.5
3	Sand	1.800	400.0	680.0
4	Clay	1.750	200.0	340.0
5	Fine sand	1.900	425.0	722.5
Bottom	Rock	1.850	600.0	1020.0

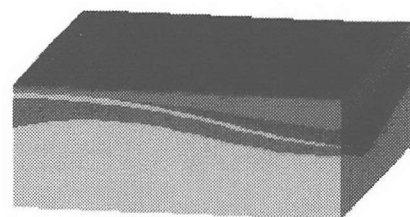
buildings located in this virtual town. The data for the structure type and height are extracted one GIS and the location is extracted from another GIS. There are WH, RC and SRC in this virtual town, and a MDOF system with estimated dynamic properties is constructed for each building. In Fig. 8, we show a bird-view of the virtual town in which a MDOF system is expressed as a bar with a common square cross section; the height of the bar is magnified by 10 times.



a) location of borehole site



b) example of interface between soil layers: fifth layer and bedrock mass



c) underground model

Figure 5. Ground structure model.



Table 4. PGV and PGD in three directions for different direction of input wave.

		EW	NS	UD
PGD [cm]	EW	3.54	0.86	0.71
	NS	0.85	4.30	0.56
	UD	0.73	0.65	2.23
PGV [kine]	EW	28.75	9.42	8.27
	NS	9.78	28.08	7.15
	UD	8.43	8.25	9.57

#### 4.1 Strong motion distribution

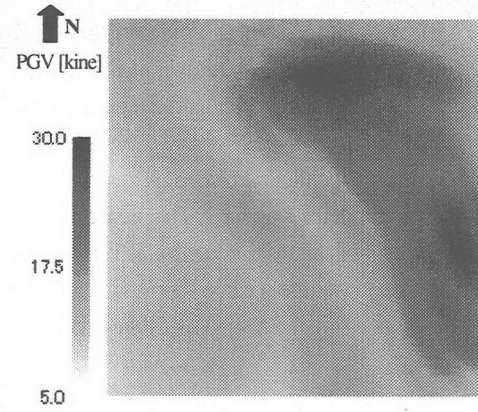
As a simple example, we input a half period sinusoid wave with 1[cm] amplitude and 5Hz frequency to the bottom layer of the virtual town. As shown later, even such a simple wave can cause complicated topographical effects on the strong motion distribution, and the resulting structure response varies from place to place. Three input waves are used in the following simulation, namely, the east-west (EW), north-south (NS) and up-down (UD) directions. Applying the micro-analysis, we compute the strong motion distribution. The spatial resolution is 2[m], and the temporal resolution is 0.001[sec] although the accuracy of numerical computation is guaranteed up to 5[Hz] is in the frequency range.

As an example of the strong motion distribution in the virtual town, the distribution of the peak ground velocity (PGV) is shown in Fig. 6. Table 4 presents the maximum value of the peak ground displacement (PGD) and the PGV for three input earthquakes. Note that the maximum value of the PGD is almost three times larger than the input earthquake. Even if the simple sinusoid wave is input, complicated distribution of the strong motion appears on the ground.

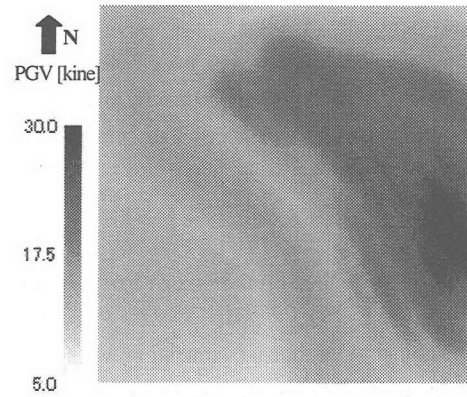
It is observed that there are two mechanisms that cause the strong motion concentration in this virtual town. The first mechanism is the amplification within soft layers; see Fig. 6 and Fig. 7. As the thickness of the surface layer increases, the PGV takes a larger value. The location of the strong motion concentration does not change much for different input waves. The second mechanism is the purely three-dimensional topographical effect. Even if the soft layer is thin, depending on the input earthquake, some parts in the virtual city take a larger value of the PGV. Thus, the location of the strong motion concentration due to this mechanism will be changed when the source earthquake is different. While the strong motion amplification due to the first mechanism is well analyzed by using the one-dimensional parallel layer models, the strong motion amplification caused by the three-dimensional topographical effects needs a full three-dimensional model of the underground structures as constructed in the present virtual town.

#### 4.2 Structure response

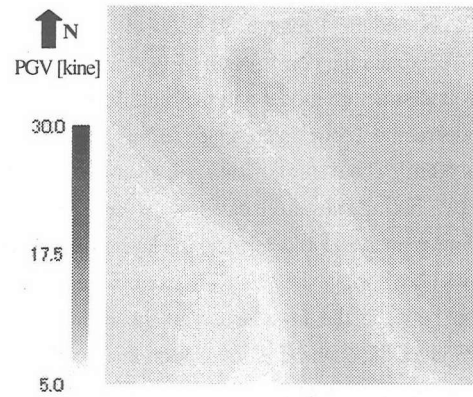
We carry out the modal analysis for around 140



a) input in EW direction



b) input in NS direction



c) input in UD direction

Figure 6. PGV distribution in virtual town.

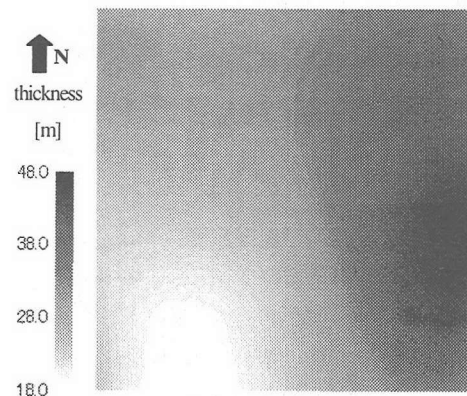


Figure 7. Distribution of thickness of soft layers.

Table 5. Structure response as the input in E-W direction.

WH			
$T_1$ [sec.]	building number	min. PD[cm]	max. PD[cm]
0.20	16	0.62	1.24
0.25	17	0.25	0.69
0.30	16	0.32	1.83
0.35	16	0.34	1.27
0.40	16	0.68	1.78
0.45	1	0.63	0.63
0.50	1	1.62	1.62
0.55	1	1.71	1.71
0.60	1	2.88	2.88
RC			
$T_1$ [sec.]	building number	min. PD[cm]	max. PD[cm]
0.21	7	0.34	0.84
0.28	10	0.31	0.93
0.35	2	0.84	1.16
0.42	2	0.87	1.08
0.56	1	3.64	3.64
0.63	2	2.53	2.66
0.70	1	2.99	2.99
0.77	2	3.38	4.61
SRC			
$T_1$ [sec.]	building number	min. PD[cm]	max. PD[cm]
0.315	7	0.66	1.58
0.420	5	0.91	1.83
0.525	5	1.74	2.34
0.630	1	1.85	1.85
0.735	4	2.63	3.34
0.840	4	3.18	9.81
0.945	1	2.57	2.57
1.155	1	11.01	11.01

Table 6. Peak displacement (PD) [cm].

a) SRC and RC					
building	type	$T_1$ [sec.]	E-W	N-S	U-D
A	SRC	1.16	11.01	12.81	2.56
B	RC	0.77	4.61	4.38	1.70
C	RC	0.77	3.38	4.20	1.44

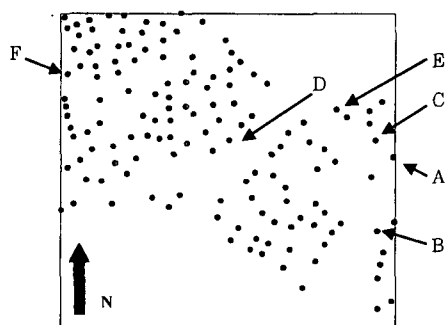
  

b) WH				
building	$T_1$ [sec.]	E-W	N-S	U-D
D	0.3	1.54	0.79	0.46
E	0.35	1.27	0.6	0.34
F	0.55	1.71	2.67	0.79

MDOF systems using the strong motion computed at the building site as the input; no soil-structure interaction is considered. This analysis is made for the three input earthquakes.

As an example of the wide distribution of the structure response, Table 5 summarizes the minimum and the maximum values of the peak displacement of buildings of the same structure type and with similar fundamental period ( $T_1$ ) when the input earthquake of the EW direction is given. As is seen, there are large differences in the structure responses; the ratio of the maximum value to the minimum value reaches almost 3. This is purely due to the fact that the input strong motion that is computed by the micro-analysis differs from place to place. Since the buildings of similar properties (the structure type and the fundamental period) have such difference, buildings of different properties have larger differences. Indeed, the ratio of the maximum value of WH to the minimum value of SRC is around 20.

We examine the wide distribution of the structure response in detail. Three *high-rise* buildings in this virtual town, which have eleven stories, are picked up. In Fig. 8, they are marked as A, B and C; A is SRC and B and C are RC. We also pick up three WH's, denoted by D, E and F in Fig. 8. Table 6 gives the peak displacement of these two groups for the three input earthquakes; a) is for A, B and C, and b) is for D, E and F, and the fundamental period ( $T_1$ ) is cited. The buildings A, B and C happen to be located at the thickest area of the soft layers. H, and hence the large strong motion is input to these buildings for all the three inputs. Still, we can observe large difference in the peak displacement; A shakes almost three times larger than B and C. For the building D, E and F, the results are more complicated. While the behaves more or less similarly to the EW input, D and E shakes less but F shakes more for the NS input. This is because large strong motion is caused for F when the EW input is given, due to the three-dimensional topographical effects. Indeed, from the comparison of Fig. 6 with Fig. 8, the concentration of the strong motion takes place



a) location of building



b) bird-view of building

Figure8. Model of buildings.

near the building F. It is clearly shown that for different earthquakes, the location of the strong motion concentration will change and hence the resulting structure responses vary almost three times.

### 5. Concluding remarks

Using the prototype of the strong motion simulator and the virtual town that is constructed from available GIS data, we carry out earthquake simulation for Roppongi area. Even though the assumed earthquake is artificial and the simplest MDOF systems are used for structural models, the simulation results clearly shows wide range of the structure responses. While it is difficult to verify the methodology of constructing the virtual town, these results support the basic validity of the methods which are developed in this paper.

For the future work, we need to construct a more realistic virtual town in which other structures such as lifelines or large infrastructure buildings are located. We seek to develop a plug-in type simulator for such a virtual town; the output of the strong motion simulator is easily input to various analysis tools of structure models, and their outputs are accumulated in a certain GIS for the virtual town.

**Acknowledge:** GIS data of Roppongi area is given by Prof. Shibasaki, Spatial Information Engineering, the University of Tokyo. For this study, we have used the computer systems of Earthquake Information Center of Earthquake Research Institute, University of Tokyo.

### REFERENCES

- 1) T. Ichimura and M. Hori: Macro-micro analysis for prediction of strong motion distribution in metropolis, *J. Struct. Eng./Earthquake Eng.*, JSCE, I-52, 654, pp. 51-62, 2000.
- 2) T. Ichimura: Development of strong motion simulator with high spatial resolution based on multi-scale analysis theory, Doctor Thesis of Department of Civil Engineering, University of Tokyo, 2001.
- 3) T. Aoyama, K. Shiono, S. Masumoto and T. Noto: Optimal determination of discontinuous surfaces, *Geoinformatics*, vol.8, no.3, pp.157-175, 1997
- 4) H. Kawakado: *Earthquake Disaster* (in Japanese), 1973.
- 5) T. Ono: *Earthquake and Anti-Seismic Building Engineering*, (in Japanese), 2001.
- 6) Kajima Research Committee of Urban Disaster Mitigation: *Techniques of Vibration Control and Reduction* (in Japanese), 1996.
- 7) Shimizu Research Committee on Building Vibration Control: *Book for Understanding of Anti-Earthquake, Vibration Reduction and Control* (in Japanese), 1999.
- 8) Mario Paz (editor): *International Handbook of Earthquake Engineering –Codes, Programs, and Examples*, New York: Chapman & Hall, 1994.
- 9) Architectural Institute of Japan: *Damping in Buildings* (in Japanese), 2000.
- 10) Anil K. Chopra: *Dynamics of Structures, Theory and Applications to Earthquake Engineering*, Prentice Hall, 2001
- 11) Ray W. Clough and Joseph Penzien: *Dynamics of Structures, Second Edition*, McGraw-Hill, Inc., 1993.

(Received: April 19, 2002)